

**Vayenas M.^a, Vaitis C.^a, Sourkouni G.^b,
Pandis P. K.^a, Argiris C.^{a,*}**^a School of Chemical Engineering,
National Technical University of Athens,
9 Iroon Polytechniou St, 15780 Zografou, Athens, Greece.^b Clausthal University of Technology,
Clausthaler Zentrum für Materialtechnik (CZM),
9 Leibnizstr., 38678 Clausthal-Zellerfeld, Germany

*e-mail: amca@chemeng.ntua.gr

Investigation of alternative materials as bifunctional catalysts for electrochemical applications

A lab-scale custom made Zinc-Air battery cell was manufactured and tested with a variety of cathode catalysts. MnO_2 has been examined both as an Oxygen Reduction Reaction (ORR) and Oxygen Evolution Reaction (OER) catalyst, with more promising results as an ORR catalyst. MnO_2 as well as a combination of MnO_2 and MWCNTs (MOCN-10) has been examined in this work. In addition, two different Metal Organic Frameworks (MOFs), specifically HKUST-1 and MOF-74, based on Cu and Ni, respectively, were investigated as an alternative and novel cathode catalyst directly on the battery cell. A power output of $20 \text{ mW} \cdot \text{cm}^{-2}$ was achieved by using MOCN-10, along with stability in prolonged discharge cycling at $5 \text{ mA} \cdot \text{cm}^{-2}$. Furthermore, MOF-loaded battery demonstrated astonishing performance in pulse cycling for more than 120 hours. Moreover, no dendrite formation was observed during long term pulse cycling.

Keywords: Rechargeable Zinc-air Battery; ORR; OER; Polarization; Cycling; MOFs

Received: 25.10.2019. Accepted: 18.11.2019. Published: 30.12.2019.

© Vayenas M., Vaitis C., Sourkouni G., Pandis P. K., Argiris C., 2019

Introduction

Advancement in energy storage systems have recently been on high demand due to the vast development of portable electronic devices, as well as to the forthcoming outburst of electrical vehicles. Lithium-ion batteries have attracted a lot of attention and have been extensively developed [1, 2]. However, high cost of raw materials used in these batteries and public safety concerns have led to explore alternative storage systems.

Zinc-air batteries (ZABs) are seen as a promising candidate for next generation energy storage devices. The needed oxygen is not stored within the ZAB and can be supplied from ambient air; therefore, they offer a high theoretical energy density of 1353 Wh/kg [3]. Zinc itself is a low-cost anode material and is also available in sufficient amounts in nature. During discharge, the zinc — air battery functions as a power generator, while electrochemical coupling of the zinc metal to the air electrode is oc-

curing in the presence of an alkaline media. Metal zinc is oxidized at the negative electrode, producing zinc cations, and the liberated electrons leave the zinc electrode and travel through an external load to the air electrode. At the same time, oxygen from the surrounding air diffuses into the porous air electrode and is ready to be reduced to hydroxide ions via the oxygen reduction reaction (ORR). ORR is occurring at the three-phase (gas oxygen, liquid electrolyte, and solid electrocatalysts) boundary as a reaction site. Generated anions OH^- then migrate from the reaction site to the zinc electrode, forming zincate ions ($\text{Zn}(\text{OH})_4^{2-}$), which at supersaturated concentrations, further decompose into insoluble zinc oxide (ZnO) [2].

Upon charging, these reactions may be reversed. The zinc — air battery is capable of storing electric energy through the oxygen-evolution reaction (OER), which is occurring at the positive electrode-electrolyte interface. At the same time, zinc is deposited at the positive electrode surface. However, the redox reactions of oxygen during the charging and discharging cycles are kinetically hindered; thus, it is common to use catalysts to accelerate the process [4].

Manganese oxide (MnO_x) has been previously reported as an efficient, cost-effective catalyst for ORR and OER catalysis [5, 6]. It is considered as a potential candidate for replacing traditional catalysts,

such as noble metals (Pt, Pd, Ru, Ir), as well as their oxides and alloys.

Metal-Organic Frameworks (MOFs) are also examined as alternative electrocatalysts [7, 8]. MOFs are hybrid crystalline materials, which consist of a metal-based centers and organic ligands. Their chemical versatility can lead to various morphologies (cubes, spheres, rods, etc.) depending on the target application. Their facile synthesis, high surface areas and open metal sites have made them highly desirable in the field of catalysis, gas storage/adsorption and gas separation, while recently they have been shown to be very promising in biomedical and electrochemical applications [9]. MOFs have been traditionally prepared via a solvothermal synthesis at high temperatures for a prolonged time (hours or even days). In order to avoid these harsh conditions, alternative methods have emerged, such as microwaves, electrochemistry, mechanochemistry and sonochemistry [10]. MOFs described in this work have been prepared by a high intensity sonicator.

In this work, a custom-made, lab-scale zinc-air battery has been constructed in order to investigate two different types of materials as catalysts. More specifically, MnO_2 -containing materials and MOF structures were used as ORR and OER electrocatalysts.

Experimental Section

Materials and Equipment

All reagents were used as received without further purification. Potassium hydroxide (KOH, purity $\geq 98\%$), Copper chloride dihydrate ($\text{CuCl}_2 \cdot 2\text{H}_2\text{O}$, purity $\geq 99\%$), 2,5-Dihydroxyterephthalic acid (dhtp, purity 98%), Ethanol (purity $\geq 98\%$), Acetone (purity $\geq 99\%$), Hydrochloric acid (HCl,

concentration 37%) were purchased from Sigma-Aldrich. Nickel nitrate hexahydrate ($\text{Ni}(\text{NO}_3)_2 \cdot 6\text{H}_2\text{O}$, purity $\geq 97\%$) was purchased from Honeywell. 1,3,5-Benzenetricarboxylic acid (Trimesic Acid, purity 98%) was purchased from Alfa-Aesar. Dimethylformamide (DMF, purity $> 99.5\%$), Methanol (purity $> 99.8\%$) were purchased from

Chem-Lab. Manganese oxide (MnO_2) was purchased from TOSOH Hellas. Nafion solution (5%) was purchased from Quin-tech. COOH Functionalized Multi-walled Carbon Nano-tubes (MWCNTs) were purchased from Hongwunematerial. Widely commercially available Zn sheets (purity > 99.9%) and Celgard-3401 membranes were also used without any modification, while carbon cloth was pretreated as described below. The sonicator used for MOF synthesis and carbon cloth pre-treatment was Vibra Cell VCX 750 W (20 KHz). The potentiostat used for electrochemical measurements was BioLogic SP-150.

Catalyst Preparation

Synthesis of Ni-MOF-74

The solution was prepared by dissolving a mixture of $\text{Ni}(\text{NO}_3)_2 \cdot 6\text{H}_2\text{O}$ (3.14 mmol) and dhtp (0.949 mmol) in a 15:1:1 mixture of DMF (75 mL), ethanol (5 mL) and deionized water (5 mL), while stirring. The mixture was transferred to a 3-neck round-bottom flask, and synthesis was carried out in a nitrogen environment via a continuous flow under ultrasound irradiation for 1 hour at a power output of 65%. After letting the vessel cool down to room temperature, the solid was recovered by centrifugation and washed once with DMF, and then with methanol. The solid was kept immersed in methanol for 4 days; the solvent was refreshed once a day. Finally, Ni-MOF-74 was activated in vacuo for 12 hours at 100 °C.

Synthesis of HKUST-1

The solution was prepared by dissolving a mixture of $\text{CuCl}_2 \cdot 2\text{H}_2\text{O}$ (3.75 mmol) and trimesic acid (3.75 mmol) in a 2:1:2 mixture of DMF (30 mL), ethanol (15 mL) and

deionized water (30 mL), while stirring. The mixture was transferred to a 3-neck round-bottom flask and synthesis was carried out in a nitrogen environment via a continuous flow under ultrasound irradiation for 1 hour at a power output of 65%. After letting the vessel cool down to room temperature, the solid was recovered by centrifugation and washed once with DMF, then with water and then ethanol within 4 days; the solid was kept immersed in water for 2 days and ethanol for 2 more days; the solvents were refreshed once a day. Finally, HKUST-1 was activated in vacuo for 12 hours at 100 °C.

Air electrode preparation

MOF catalysts were used as prepared and described above, MnO_2 was used as purchased, while MnO_2 -MWCNTs combination was prepared by mixing 18 mg MnO_2 and 2 mg MWCNTs. In order for as-prepared catalysts to be loaded on cathode, 20 mg of each catalyst were dispersed in 1 ml ethanol and underwent sonication in an ultrasound bath for 10 min. 150 μl of Nafion solution (5%) were also added and the final mixture was sonicated for 10 min. Finally, the dispersion was poured onto a pretreated carbon cloth (1.5 cm \times 1.5 cm).

Carbon cloth pre-treatment

The catalyst support used for our battery cells was sonicated in three different solutions before being loaded by the catalyst [11]. Carbon cloth (1.5 cm \times 1.5 cm) was successively immersed into 20% HCl, acetone and deionized water. Each sonication lasted 15 min with a power output of 33%, while the carbon cloth was fully immersed.

Results and discussion

Different types of materials were prepared as described above in order to be

examined as Zn-air battery electrocatalysts. MnO_2 and MOCN-10 (mixture of MnO_2

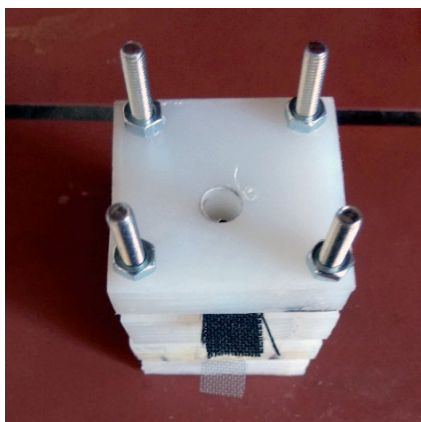


Fig. 1. Photograph of zinc-air battery

and MWCNTs) were electrochemically compared with each other. Furthermore, MOF structures were also examined as electrocatalysts. As-prepared catalysts were directly loaded on carbon cloth in order to catalytically activate the three-phase boundaries.

A home-made rechargeable Zn-air battery was built (see Fig. 1) to evaluate the performance of as-prepared electrocatalysts of the air electrode. In Fig. 2a, a stable Open Circuit Voltage (OCV) is exhibited regardless using MnO_2 or MnO_2 -CNTs catalysts. OCV for MnO_2 catalyst cell is equal to 1.48 V, while 1.44 V OCV is monitored for MOCN-10 catalyst.

Fig. 2b shows the galvanodynamic polarization curves of batteries loaded with MnO_2 and MOCN-10 catalysts on the anode. The exhibited potential is monitored for increasing current density, while charging (positive current) or discharging (negative current) the cell with a scan rate of $0.5 \text{ mA} \cdot \text{sec}^{-1}$.

Corresponding power curves for cells using different air catalysts are depicted in Fig. 2c. MOCN-10 catalyst shows the highest power pick at 20 mW/cm^2 . Energy efficiency curve for the same battery was also calculated by dividing the values

of charge polarization by the values of discharge polarization. Comparing to the corresponding power curve, it is apparent that the energy efficiency is reduced to 29.1% while power peak is observed. That means that the battery's energy efficiency has been reduced by 70.9% (see Fig. 2d).

To evaluate the cycling stability of the battery, a low current density of $2 \text{ mA} \cdot \text{cm}^{-2}$ was first applied for pulsed and non-pulsed cycles. During non-pulsed cycling, $2 \text{ mA} \cdot \text{cm}^{-2}$ were applied for 2 h of charging and $4 \text{ mA} \cdot \text{cm}^{-2}$ were applied for 1 h of discharging while 13 cycles were obtained without any obvious deterioration. Therefore, the capacity output was equal for charge and discharge. The different currents applied are due to the better ORR activity of various manganese oxide forms compared to the OER [5]. With the utilization of MnO_2 as a catalyst, cell potential during the ORR process was 1.10 V, while the respective potential during OER process was 2.00 V (see Fig. 3 a, b). Surprisingly, both the ORR and OER potentials of the MOCN-10 battery were 1.20 V and 2.10 V, respectively (see Fig. 3 c, d). However, for both catalysts the voltage gap was equal. A charge-discharge voltage gap ($\Delta\eta$) of less than 900 mV has been

observed while cycling regardless of the air catalyst.

Fig. 4 shows a discharge profile plot for the cell where MOCN-10 acted as the cathode catalyst. After increasing the current density on 20 mA/cm² discharge and successively reducing the applied current density until 0.5 mA/cm², only 49 mV reduction has been observed, corresponding to 96.2% potential retention.

Furthermore, MOF crystals were examined as ORR and OER catalysts directly on Zn-air batteries. Due to their high porosity and large surface areas, MOFs can contrib-

ute to the reaction area between the three-phase sites on cathode.

Utilization of HKUST-1 as air catalyst shows increased battery performance, as the battery is able to remarkably perform for over 350 consecutive cycles on pulse charging of 20 min without any apparent deterioration (see Fig. 5). Battery cell using Ni-MOF-74 has also been evaluated through galvanostatic cycling (see Fig. 6). However, the observed $\Delta\eta$ between charging and discharging is greater than 1 V.

In Fig. 7, Zn sheets that have been used during cycling can be seen. The formation

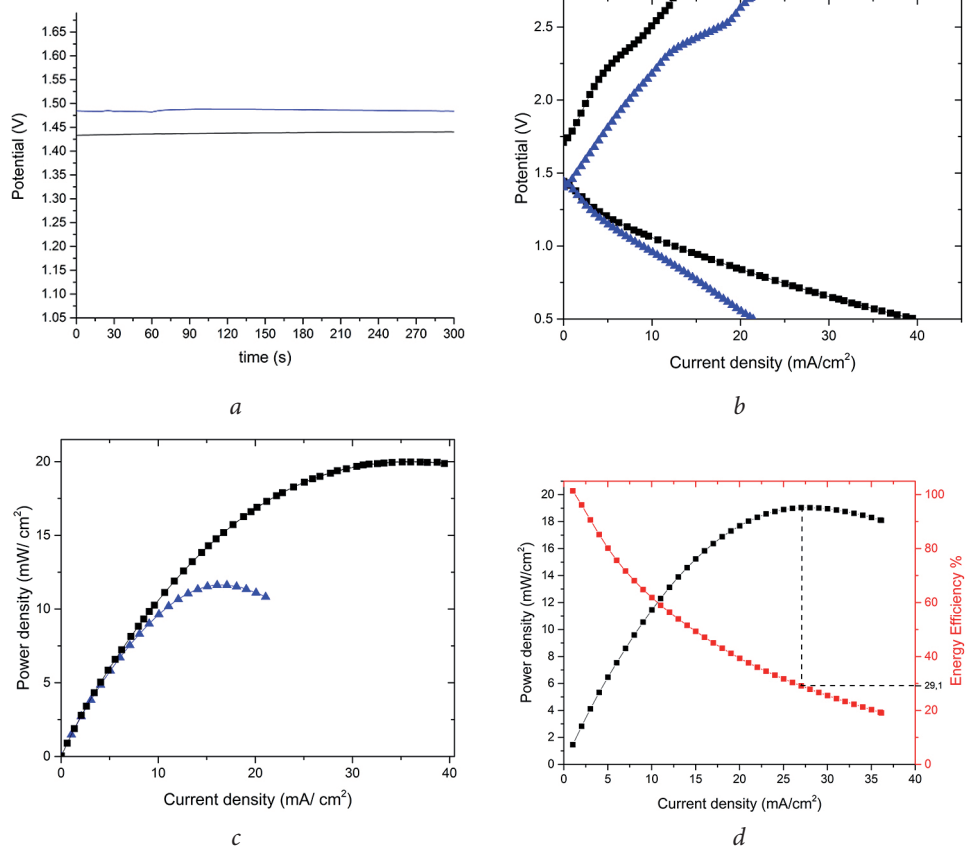


Fig. 2. Electrochemical performance of Zinc-air batteries using MnO₂ (blue) and MnO₂-CNTs (black) as air catalysts: *a* — OCV plots; *b* — Polarization curves and *c* — the corresponding power density; *d* — Energy efficiency curve for MOCN-10 cell (red) regarding its power density curve (black) vs current density

of ZnO structures that increase the polarization and lead to degradation can easily be observed [12, 13]. Although, much less

ZnO formed during pulsed cycling than during non-pulsed cycling, even if the total time of pulsed cycling was longer.

Conclusions

In this work, a lab scale rechargeable zinc-air battery has been developed, and different material structures have been investigated as ORR and OER catalysts. MnO_2 has already been reviewed in the literature as an excellent ORR catalyst, but further testing needs to be done for the OER catalytic process. Hereby, we prepared MnO_2 and MWCNTs mixture — loaded cathode

and compare the respective battery's performance with the MnO_2 loaded battery. Relative to MnO_2 — loaded cells, battery cells with MOCN-10 mixture show higher power output. In particular, we achieved $20 \text{ mW} \cdot \text{cm}^{-1}$ utilizing the MnO_2 -CNTs mixture as air catalyst for ORR and OER.

Additionally, MOF structures were evaluated as catalysts. Cathode was pre-

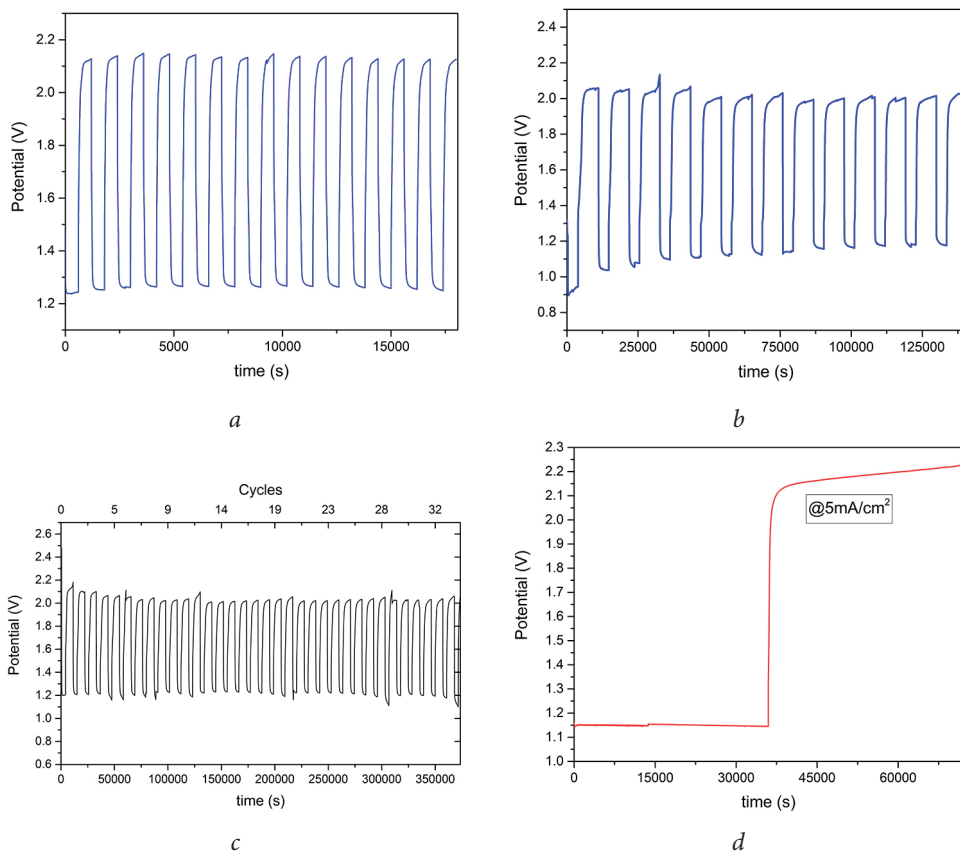


Fig. 3. *a* — Discharge and charge cycling at $2 \text{ mA} \cdot \text{cm}^{-2}$ for cell with MnO_2 as electrocatalyst; *b* — Discharge (at $4 \text{ mA} \cdot \text{cm}^{-2}$) and charge (at $2 \text{ mA} \cdot \text{cm}^{-2}$) cycling for cell with MnO_2 as electrocatalyst; *c* — Discharge (at $4 \text{ mA} \cdot \text{cm}^{-2}$) and charge (at $2 \text{ mA} \cdot \text{cm}^{-2}$) cycling for cell with MOCN-10 as electrocatalyst; *d* — Discharge and charge at $5 \text{ mA} \cdot \text{cm}^{-2}$ of MOCN-10 loaded cell

pared in the same way as with MnO_2 catalysts and Nafion acted as binder between catalyst and Gas Diffusion Layer (GDL). Galvanodynamic polarization curves in the MOF-loaded cell, with current step of $0.5 \text{ mA} \cdot \text{s}^{-1}$, showed performance comparative to that of the MnO_2 catalysts. In particular, battery cell with HKUST-1 on the cathode, performed at $7 \text{ mW} \cdot \text{cm}^{-1}$ and surpassed the $3.5 \text{ mW} \cdot \text{cm}^{-1}$ power output of Ni-MOF-74 loaded cell. What is more, great cycling stability has been achieved during short cycles (pulsed cycling). While utilizing HKUST-1 cell, more than 360 successive cycles (120 hrs) were

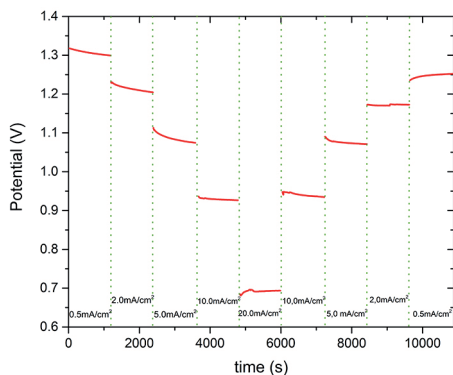


Fig. 4. Discharge profile of the battery cell with MnO_2 -CNTs air catalyst for 0.5, 2, 5, 10 and $20 \text{ mA} \cdot \text{cm}^{-2}$ and vice versa

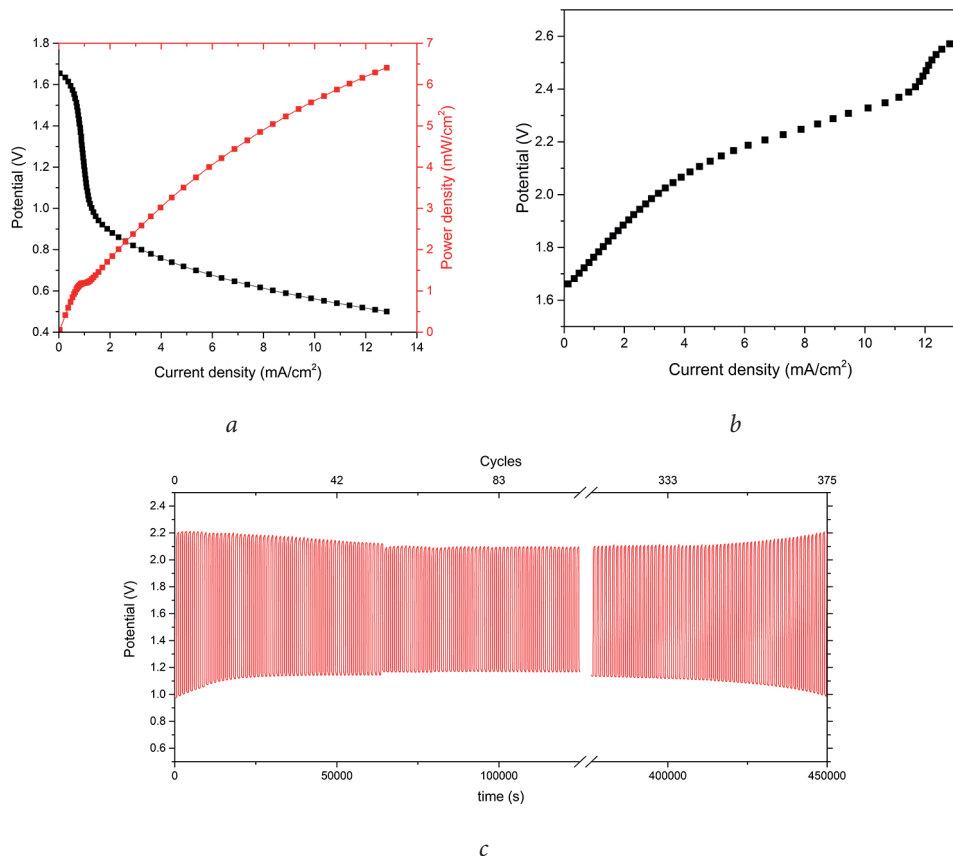


Fig. 5. Electrochemical performance of Zinc-air batteries using HKUST-1 as air catalyst: *a* — Discharge polarization curve and the corresponding power curve; *b* — Charge polarization curve; *c* — Discharge and charge cycling at $2 \text{ mA} \cdot \text{cm}^{-2}$

performed at $2 \text{ mA} \cdot \text{cm}^{-1}$ without deterioration of the cell, indicating great stability during both ORR and OER operation.

In the future, more MOF structures might be candidates for utilization as air catalysts including Mn-based MOFs.

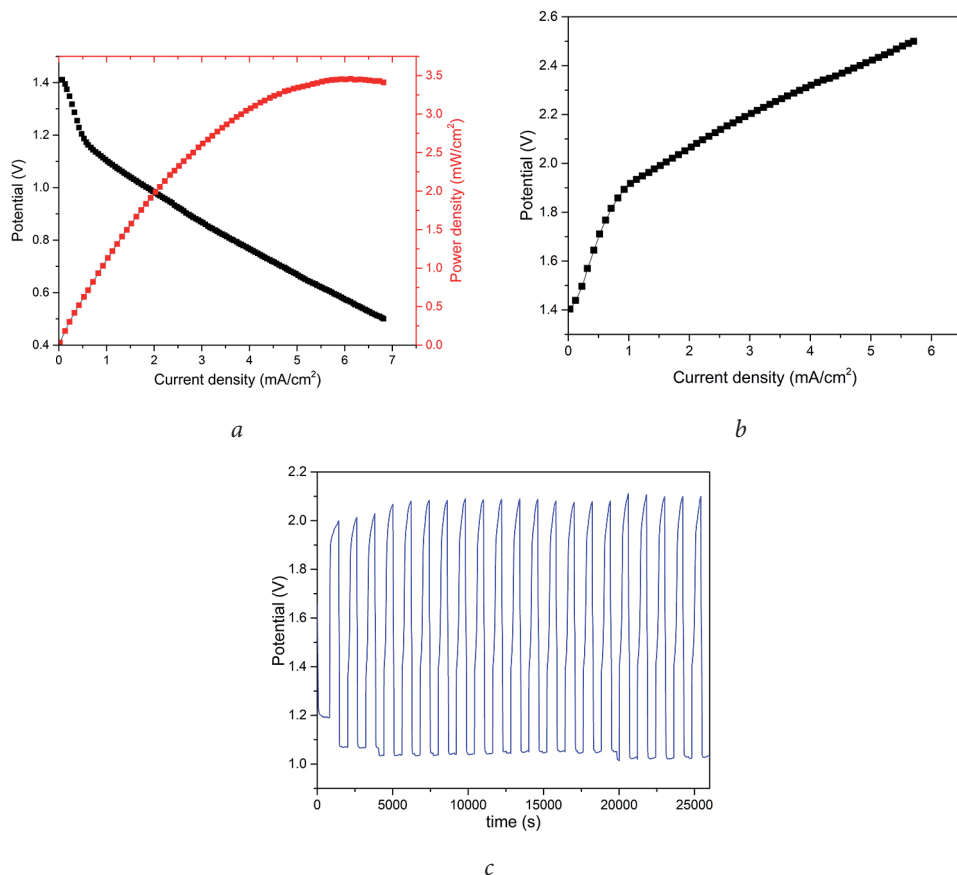


Fig. 6. Electrochemical performance of Zinc-air batteries using Ni-MOF-74 as air catalyst: *a* — Discharge polarization curve and the corresponding power curve; *b* — Charge polarization curve; *c* — Discharge and charge cycling at $2 \text{ mA} \cdot \text{cm}^{-2}$

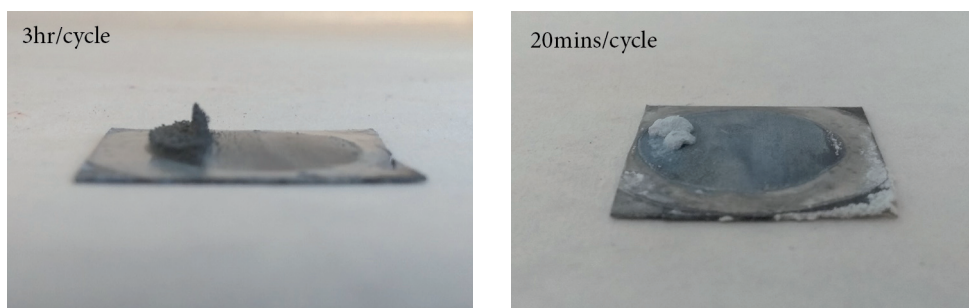


Fig. 7. Zinc electrode after cycling performance for long and pulse cycling at $2 \text{ mA} \cdot \text{cm}^{-2}$

References

1. Menictas C. *Advances in batteries for medium and large-scale energy storage*. Boston, MA: Elsevier; 2015.
2. Reddy T, Linden D. *Linden's Handbook of Batteries (4th Edition)*. New York, USA: McGraw-Hill Professional Publishing; 2010.
3. Fu J, Cano ZP, Park MG, Yu A, Fowler M, Chen Z. Electrically Rechargeable Zinc-Air Batteries: Progress, Challenges, and Perspectives. *Advanced Materials*. 2017;29(7):1604685.
DOI:10.1002/adma.201604685
4. Xiong M, Clark MP, Labbe M, Ivey DG. A horizontal zinc-air battery with physically decoupled oxygen evolution/reduction reaction electrodes. *Journal of Power Sources*. 2018;393:108–18.
DOI:10.1016/j.jpowsour.2018.05.004
5. Sumboja A, Ge X, Goh FWT, Li B, Geng D, Hor TSA, et al. Manganese Oxide Catalyst Grown on Carbon Paper as an Air Cathode for High-Performance Rechargeable Zinc-Air Batteries. *ChemPlusChem*. 2015;80(8):1341–6.
DOI:10.1002/cplu.201500183
6. Sumboja A, Ge X, Zheng G, Goh FWT, Hor TSA, Zong Y, et al. Durable rechargeable zinc-air batteries with neutral electrolyte and manganese oxide catalyst. *Journal of Power Sources*. 2016;332:330–6.
DOI:10.1016/j.jpowsour.2016.09.142
7. Zhao R, Liang Z, Zou R, Xu Q. Metal-Organic Frameworks for Batteries. *Joule*. 2018;2(11):2235–59.
DOI:10.1016/j.joule.2018.09.019
8. Wang Z, Hu J, Han L, Wang Z, Wang H, Zhao Q, et al. A MOF-based single-ion Zn²⁺ solid electrolyte leading to dendrite-free rechargeable Zn batteries. *Nano Energy*. 2019;56:92–9.
DOI:10.1016/j.nanoen.2018.11.038
9. Butova VV, Soldatov MA, Guda AA, Lomachenko KA, Lamberti C. Metal-organic frameworks: structure, properties, methods of synthesis and characterization. *Russian Chemical Reviews*. 2016;85(3):280–307.
DOI:10.1070/rcr4554
10. Vaitsis C, Sourkouni G, Argirusis C. Metal Organic Frameworks (MOFs) and ultrasound: A review. *Ultrasonics sonochemistry*. 2019;52:106–19.
DOI:10.1016/j.ultsonch.2018.11.004
11. Mou K, Chen Z, Yao S, Liu L. Enhanced electrochemical reduction of carbon dioxide to formate with in-situ grown indium-based catalysts in an aqueous electrolyte. *Electrochimica Acta*. 2018;289:65–71.
DOI:10.1016/j.electacta.2018.09.026
12. Cheng Y, Zhang L, Xu S, Zhang H, Ren B, Li T, et al. Ionic liquid functionalized electrospun gel polymer electrolyte for use in a high-performance lithium metal battery. *J Mater Chem A*. 2018;6(38):18479–87.
DOI:10.1039/C8TA06338A

13. Jin Y, Chen F. Facile preparation of Ag-Cu bifunctional electrocatalysts for zinc-air batteries. *Electrochimica Acta*. 2015;158:437–45.
DOI:10.1016/j.electacta.2015.01.151